Signature of CEF-phonon coupling in Kondo lattice system CeCuGa3

Anand, V.K.; Fraile, Alberto; Adroja, D.T.; Sharma, Shivani; Tripathi, Rajesh; Ritter, C.; de la Fuente, C.; Biswas, P.K.; Sakai, V. Garcia; del Moral, A.; Strydom, A.M.

Journal of Physics: Conference Series

Published: 01/03/2022

Publisher's PDF, also known as Version of record

PAPER • OPEN ACCESS

Signature of CEF-phonon coupling in Kondo lattice system $CeCuGa_3$

To cite this article: V K Anand *et al* 2022 *J. Phys.: Conf. Ser.* **2164** 012056

Signature of CEF-phonon coupling in Kondo lattice system $CeCuGa_3$

V K Anand[1,2], A Fraile[3] D T Adroja[1,4], Shivani Sharma[1], Rajesh Tripathi[1,5], C Ritter[6], C de la Fuente[7], P K Biswas[1], V Garcia Sakai[1], A del Moral[7] and A M Strydom[4]

[1]ISIS Facility, Rutherford Appleton Laboratory, Chilton, Didcot, Oxon, OX11 0QX, United Kingdom
[2]Department of Physics, University of Petroleum and Energy Studies, Dehradun, Uttarakhand, 248007, India
[3]Nuclear Futures Institute, Bangor University, Bangor, LL57 1UT, UK
[4]Highly Correlated Matter Research Group, Physics Department, University of Johannesburg, P.O. Box 524, Auckland Park 2006, South Africa
[5]Jawaharlal Nehru Centre for Advanced Scientific Research, Jakkur, Bangalore 560064, India
[6]Institut Laue-Langevin, Boite Postale 156, 38042 Grenoble Cedex, France
[7]Departamento de Fisica de Materia Condensada, Facultad de Ciencias, Universidad de Zaragoza, E-50009 Zaragoza, Spain

E-mail: vivekkranand@gmail.com, devashibhai.adroja@stfc.ac.uk

Abstract. We present the results of inelastic neutron scattering (INS) measurements on Kondo lattice heavy fermion $CeCuGa_3$. The low-temperature magnetic susceptibility exhibits an anomaly near 2.6 K associated with an antiferromagnetic transition which is further confirmed by the heat capacity measurement. The analysis of magnetic heat capacity $C_{\rm mag}(T)$ based on the crystal electric field (CEF) model reveals an overall CEF splitting of $\sim$ 21 meV. The INS data reveal two strong magnetic excitations near 4.5 and 6.9 meV, which, however failed to reproduce the observed $C_{\rm mag}(T)$. We therefore analyze the INS data by a model based on magneto-elastic (i.e. CEF-phonon) coupling which suggests that the excitations observed near 4.5 and 6.9 meV originate from the CEF-phonon coupling as observed in $CeCuAl_3$ and $CeAuAl_3$.

1. Introduction

Crystal electric field (CEF) effect plays an important role in dictating the physical properties of rare-earth intermetallic compounds. Among the rare-earth intermetallics, Ce-compounds are well known to present diverse physical properties [1-3]. The electronic ground state of a Ce-compound is determined by competing RKKY, Kondo and crystal electric field (CEF) interactions. Ce^{3+} ($4f^1$) with $J = 5/2$ has six-fold degenerate ground state multiplet which when subject to CEF environment (lower than a cubic point symmetry) splits into three doublets. As specified by Kramer's degeneracy theorem, being a Kramers ion, for Ce^{3+} one would expect only two CEF excitations from the ground state in the paramagnetic state for a low point symmetry. In this regard recent observations of three CEF excitations in some of the tetragonal Ce-compounds such as $CeCuAl_3$ [4] and $CeAuAl_3$ [5] are quite striking, and provide evidence for strong CEF-phonon coupling (magneto-elastic coupling) in these compounds.

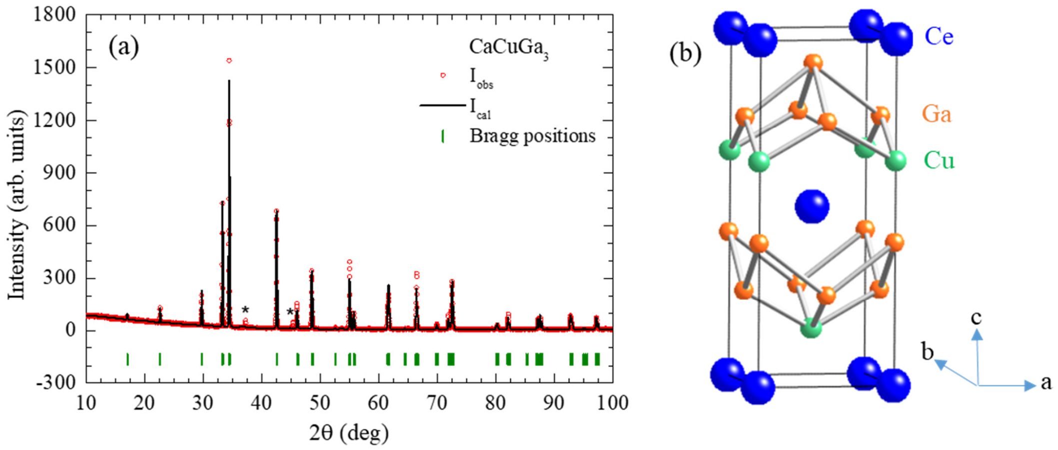

Figure 1. (a) Room temperature x-ray powder diffraction pattern of $CeCuGa_3$ along with the structural refinement profile for noncentrosymmetric $BaNiSn_3$-type tetragonal structure (space group $I4mm$). The short vertical bars indicate the Bragg peak positions. Asterisks mark the unidentified impurity peaks. (b) The unit cell representing the $BaNiSn_3$-type noncentrosymmetric tetragonal (space group $I4mm$) crystal structure of $CeCuGa_3$.

Here we present another tetragonal compound, namely $CeCuGa_3$, which shows signature of CEF-phonon coupling. Earlier investigations on Kondo lattice heavy fermion $CeCuGa_3$ [6-14] have shown a sample dependent ground state. Depending on Cu/Ga stoichiometry as well as crystal structure, different groups have reported different magnetic states, such as paramagnetic behavior down to 0.4 K [7], antiferromagnetic (AFM) ordering below 1.9 K [8, 10] and ferromagnetic ordering below 4 K [13]. It was suggested that it is the degree of Cu-Ga disorder that plays a key role in adapting the crystal structure, whether $ThCr_2Si_2$-type tetragonal structure ($I4/mmm$) or $BaNiSn_3$-type tetragonal structure ($I4mm$), and controls the ground state properties of $CeCuGa_3$.

2. Experimental

A polycrystalline sample of $CeCuGa_3$ was prepared by standard arc-melting on water-cooled copper hearth under inert atmosphere. In order to homogenize, the arc-melted button was flipped and re-melted several times, and annealed at 900° C for a week. The quality of sample was checked by room temperature x-ray diffraction (XRD) on powdered sample. Magnetic susceptibility χ vs temperature T was measured by a commercial superconducting quantum interference device (SQUID) magnetometer (MPMS, Quantum Design). The heat capacity $C_{\rm p}(T)$ was measured by relaxation method using a physical properties measurements system (PPMS, Quantum Design). The inelastic neutron scattering measurement was performed on the MARI time of flight spectrometer at the ISIS Facility, UK. The powdered sample was wrapped in thin Al-foils and mounted inside a thin-walled cylindrical Al-can which was then cooled down to 4.7 K in a top-loading closed cycle refrigerator with He-exchange gas. The INS data were collected at 4.7 K and 100 K using neutrons with incident energies $E_i = 15$ and 40 meV.

3. Results and Discussion

Crystallography and the sample quality were checked by room temperature x-ray powder diffraction. The powder XRD pattern is shown in Fig. 1(a). The XRD data were refined by Rietveld refinement using the software FullProf. The structural Rietveld refinement profile fit for the noncentrosymmetric $BaNiSn_3$-type tetragonal structure (space group $I4mm$) is shown

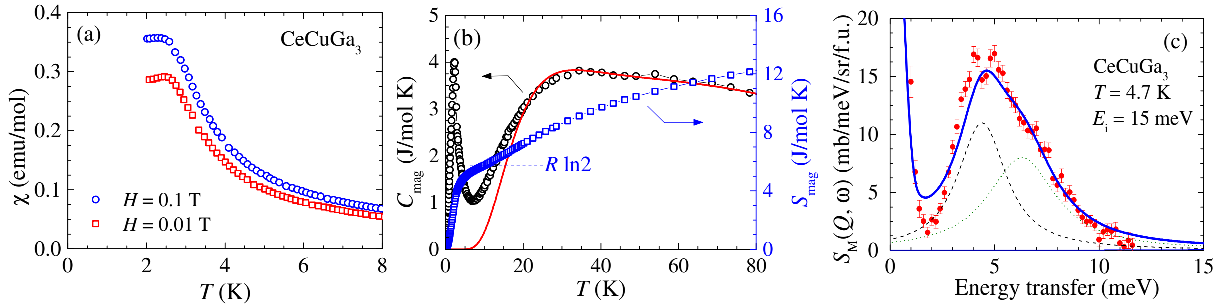

Figure 2. (a) The low temperature magnetic susceptibility χ versus temperature T of $CeCuGa_3$ measured in applied fields $H = 0.01$ and 0.1 T. (b) Magnetic contributions to heat capacity $C_{\rm mag}(T)$ and magnetic entropy $S_{\rm mag}(T)$. The solid red curve represents the Schottky contribution to $C_{\rm mag}$ due to crystal electric field (CEF). (c) Q-integrated ($0 \leq Q \leq 2.5$ Å^{-1}) inelastic magnetic scattering intensity $S_{\rm M}(Q,\omega)$ versus energy transfer E measured with $E_i =$ 15 meV at 4.7 K. The solid blue curve represents the fit of the INS data based on magneto-elastic CEF-phonon coupling model. The dashed and dotted curves represent the two excitations.

in Fig. 1(a). An almost single phase nature of sample is inferred from the XRD data and fit. The XRD also shows the presence of a tiny amount of unidentified impurity in the sample, the impurity peaks are marked with asterisks in Fig. 1(a). The refinement yielded the lattice parameters $a = 4.2533(1)$ Å and $c = 10.4497(2)$ Å which are in very good agreement with the literature values [10]. In $BaNiSn_3$-type tetragonal structure the atoms Ce, Cu, Ga1 and Ga2 occupy the Wyckoff positions 2a $(0,0,0)$, 2a $(0,0,z_{\rm Cu})$, 2a $(0,0,z_{\rm Ga1})$, and 4b $(0,0,z_{\rm Ga2})$, respectively. The values of the z-coordinates obtained from the refinement are $z_{\rm Cu} = 0.597(2)$, $z_{\rm Ga1} = 0.373(2)$, and $z_{\rm Ga2} = 0.259(2)$. The $BaNiSn_3$-type noncentrosymmetric tetragonal structure of $CeCuGa_3$ is shown in Fig. 1(b). As can be seen from Fig. 1(b), this structure lacks an inversion symmetry along the c-axis.

Figure 2(a) shows the low-T $\chi(T)$ data measured in magnetic fields $H = 0.01$ and 0.1 T. At $H = 0.01$ T $\chi(T)$ exhibits an anomaly near 2.6 K which shifts to 2.5 K as H is increased to 0.1 T, suggesting an antiferromagnetic transition. Above 100 K, the $\chi(T)$ follows a modified Curie-Weiss behavior $\chi = \chi_0 + C/(T-\theta_{\rm p})$ with $\chi_0 = 4.8 \times 10^{-4}$ emu/mol, effective moment $\mu_{\rm eff} = 2.37\,\mu_{\rm B}$ and Weiss temperature $\theta_p = -18(2)$ K [15]. The value of $\mu_{\rm eff}$ is close to the theoretical value of $2.54\,\mu_{\rm B}$/Ce expected for Ce^{3+} ions. An AFM transition is also inferred from the heat capacity data which shows a sharp λ-type anomaly near 2.3 K. The magnetic contribution to heat capacity $C_{\rm mag}(T)$ obtained after subtracting the phonon contribution (equivalent to heat capacity of nonmagnetic reference $LaCuGa_3$ [15]) is shown in Fig. 2(b) along with the magnetic entropy $S_{\rm mag}(T)$. The AFM ordering is further confirmed by muon spin relaxation and neutron powder diffraction (NPD) measurements [15]. The NPD reveals an incommensurate magnetic structure described by wave vector $\mathbf{k} = (0.148, 0.148, 0)$ corresponding to a longitudinal spin density wave with ordered moments in the ab-plane [15]. In addition to λ-type anomaly, $C_{\rm mag}(T)$ also presents a broad Schottky-type anomaly associated with crystal electric field. We analyzed the $C_{\rm mag}(T)$ by a three-level CEF scheme [16, 17] [see Fig. 2(b)] which suggests that with an oveall splitting of 240 K, the first excited doublet lies 70 K above the ground state. The splitting energy of 70 K obtained so is consistent with $S_{\rm mag}(T)$ which attains a value of $R\ln 4$ near 66 K [Fig. 2(b)]. The CEF level scheme deduced so is consistent with the one obtained from the analysis of single crystal $\chi(T)$ by Joshi *et al.* [13].

Figure 2(c) shows the Q-integrated ($0 \leq Q \leq 2.5$ Å^{-1}) one-dimensional energy cut of magnetic contribution $S_M(Q,\omega)$ to INS response of $CeCuGa_3$ at 4.7 K. A relatively broad CEF excitation consisting of two closely situated magnetic excitations is seen. We analyzed the INS data by a model based on crystal field, the CEF Hamiltonian for Ce^{3+} ions in tetragonal symmetry is given by $H_{\rm CEF} = B_2^0 O_2^0 + B_4^0 O_4^0 + B_4^4 O_4^4$, where B_n^m represent the CEF parameters and O_n^m the Stevens operators [18]. Our analysis of INS data by this model suggests two closely situated CEF excitations at 4.5 and 6.9 meV. The overall splitting of 6.9 meV in this model is much lower than the value 20.7 meV (240 K) inferred above from the analysis of $C_{\rm mag}(T)$. Joshi *et al.* [13] also suggested an overall splitting of 19.6 meV (228 K) from the analysis of $\chi(T)$. Further, the CEF parameters obtained fail to explain the $\chi(T)$ and $C_{\rm mag}(T)$ data. This inconsistency suggests that the 4.5 and 6.9 meV excitations do not originate only from single-ion CEF transition, and very likely results from the splitting of a CEF level due to CEF-phonon coupling. We therefore analyzed the INS data by a model based on magneto-elastic (CEF-phonon) coupling model, i.e., by including the magneto-elastic as well as CEF-phonon terms to the Hamiltonian, such that $H_{\rm tot} = H_{\rm CEF} + H_{\rm CEF-ph} + H_{\rm MEL}$, with $H_{\rm CEF-ph} = \hbar\omega_0(a_u^+ a_u + 1/2)$ and $H_{\rm MEL} = M^\gamma(a_u + a_u^+)O_u$ [4, 15]. The analysis of INS data by this model suggests three CEF excitations at 4.6, 7.2 and 28.2 meV. The calculated intensity of 28.2 meV excitation is very weak, which also agrees with our 40 meV INS data [15]. The fit of INS data by this model is shown by solid blue curve in Fig. 2(c) along with the contributions from individual excitations at 4.6 and 7.2 meV. The CEF parameters obtained from the CEF-phonon model also explain very well the anisotropic behaviour of single crystal $\chi(T)$, and $C_{\rm mag}(T)$ data [15].

4. Conclusion

We have investigated the crystal field states of $CeCuGa_3$ using inelastic neutron scattering and heat capacity measurements. The analysis of INS data by a model based on CEF suggests two excitations near 4.5 and 6.9 meV. On the other hand, $C_{\rm mag}(T)$ suggests an overall CEF splitting of 20.7 meV. We therefore analyzed the INS data by a model based on magneto-elastic (CEF-phonon) coupling which suggests that the 4.5 and 6.9 meV excitations originate from CEF-phonon coupling similar to the homologue compounds $CeCuAl_3$ and $CeAuAl_3$.

References

[1] Stewart G R 1984 *Rev. Mod. Phys.* **56** 755; Stewart G R 2001 Rev. Mod. Phys. **73** 797; Stewart G R 2006 Rev. Mod. Phys. **78**, (2006) 743.
[2] Löhneysen H v, Rosch A, Vojta M and Woelfle P 2007 *Rev. Mod. Phys.* **79** 1015
[3] Pfleiderer C 2009 *Rev. Mod. Phys.* **81** 1551
[4] Adroja D T, Moral A del, Fuente C de la, Fraile A, Goremyhkin E A, Taylor J W, Hillier A D and Fernandez-Alonso F 2012 *Phys. Rev. Lett.* **108** 216402
[5] Čermák P, Schneidewind A, Liu B, Koza M M, Franz C, Schönmann R, Sobolev O and Pfleiderer C 2019 *Proc. Natl. Acad. Sci.* **116** 6695
[6] Sampathkumaran E V and Das I 1992 *Solid State Commun.* **81** 901
[7] Mentink S A M, Bos N M, van Rossum B J, Nieuwenhuys G J, Mydosh J A and Buschow K H J, J. Appl.Phys. **73**, 6625 (1993).
[8] Martin J M, Paul D M, Lees M R, Werner D and Bauer E, J. Magn. Magn. Mater. **159**, 223 (1996).
[9] Aoyama S, Ido H, Nishioka T, Kontani M 1996 *Czechoslov. J. Phys.* **46** 2069
[10] Martin J M, Lees M R, Paul D M, Dai P, Ritter C and Bi Y J 1998 *Phys. Rev. B* **57** 7419
[11] Kontani M, Motoyama G, Nishioka T and Murase K 1999 *Physica B* **259**, 24
[12] Oe K, Kawamura Y, Nishioka T, Kato H, Matsumura M and Kodama K 2010 *J. Phys.: Conf. Ser.* **200** 012147
[13] Joshi D A, Burger P, Adelmann P, Ernst D, Wolf T, Sparta K, Roth G, Grube K, Meingast C and Löhneysen H v 2012 *Phys. Rev. B* **86** 035144
[14] Przybylski P, Pikul A P, Kaczorowski D, Wiśniewski P 2014 *J. Phys. Chem. Solids* **75** 1284
[15] Anand V K *et al.* (to be published)
[16] Layek S, Anand V K and Hossain Z 2009 *J. Magn. Magn. Mater.* **321** 3447
[17] Anand V K, Adroja D T, Britz D, Strydom A M, Taylor J W and Kockelmann W 2016 *Phys. Rev. B* **94** 014440
[18] Stevens K W H 1952 *Proc. Phys. Soc. London A* **65** 209